The Korean Journal of Ceramics, **4** [4] 356 - 362 (1998)

Hertzian Crack Suppression and Damage Tolerance of Silicon Nitride Bilayer

Kee Sung Lee, Do Kyung Kim, Seung Kun Lee* and Brian R. Lawn*

Dept. of Materials Science and Engineering, KAIST, Taejon, 305-701, Korea
**Materials Science and Engineering Laboratory,*
National Institute of Standards and Technology, Gaithersburg, MD20899, USA
(Received September 23, 1998)

Hertzian crack suppression phenomena and relatively high damage tolerance were investigated in hard/soft silicon nitride (Si_3N_4) bilayers. Coarse α-Si_3N_4 powder was used for the hard coating layer and fine α-Si_3N_4 powder was used for the soft substrate layer. The two layers were designed with a strong interface. Hertzian indentation was used to investigate contact fracture and damage tolerance property. Hertzian crack suppression has occurred with increasing applied load and decreasing coating thickness. The crack suppression contributed strength improvement, especially in the bilayers with thinner coatings. Ultimately, the combination of hard coating with soft but tough underlayer improved the damage tolerance of brittle Si_3N_4 ceramics.

Key Words : Bilayer, Hertzian crack Suppression, Hertzian indentation, Residual stress, Silicon nitride

I. Introduction

In brittle material such as ceramics, an applied stress is usually concentrated on the tip of flaws in the material. Material near the crack tip is loaded to higher stresses than any other surrounding materials. Experimental fracture strengths for brittle materials are much lower than theoretical cohesive strength, $E/10$ (E: Young's modulus). Griffith found that the typical brittle solid contains a profusion of submicroscopic flaws.[1,2] In the development of high strength and toughened ceramics, most research can be divided into two approaches. One is a method which inhibits the crack initiation, and the other relates to crack suppression (resistance of crack growth). The first approach deals mainly with the elimination of flaws.[3,4] However, it is very difficult to eliminate flaws completely. Even if the material was fabricated without flaws, it may develop small flaws during the shaping of brittle material by cutting, grinding, abrasion, and drilling. Damage and subsequent wear of the material occasionally cause production of flaws. Therefore, the direction of research in this field has moved to the second approach.[4,5] According to the second approach, cracks hardly propagate even though flaws exist. Flaw insensitivity is related to the stabilization of crack growth by microstructure shielding such as large and elongated grains, high internal stresses, and weak interfaces.[6,7] It is well recognized that the microstructure is profoundly controllable by suitable heat treatments or starting powders.[8-11] Flaw insensitivity or damage tolerance is a desirable property in brittle ceramics from the point of view of material design. It enables the material engineer to design protection from brittleness irrespective of existing critical flaws in the material.

However, in controlling self-microstructure factors, high toughness can cause deterioration of wear or fatigue properties.[8,12] Even if elongated grain structures give rise to enhanced long-crack toughness, the toughness in the short-crack domain may be diminished, where important properties such as strength and wear are determined. There is a contradiction in the development of ceramics with both high wear resistance and high toughness. Due to this fact, ceramic laminates have been recently developed.[13] The ceramic laminate provides new mechanical properties because it has layers with different microstructures. The advantage of laminates is that they can be tailored to specific applications because the properties can be manipulated for the appropriate layer design. Another advantage is that they contribute flaw insensitivity by controlling the interfacial strength[14-16] or residual stress.[17,18]

Our principal aim is to design highly reliable Si_3N_4 bilayer which suppresses rather than deflects cracks. The approach is to develop a ceramic layer structure with superior property combinations through a novel concept of layered homogeneous/heterogeneous microstructures with relatively hard surfaces (coatings) on soft underlayers (substrates). An important concept is the incorporation of a small interlayer elastic/plastic mismatch.[19] A strong interface was introduced in order to not only suppress delamination but also distribute applied energy into the damage absorbent underlying layer. The two Si_3N_4 layers are fabricated from different starting powders from relatively coarse and fine α-Si_3N_4 phase powder. The

coarse and essentially equiaxed α-Si_3N_4 grains show slow transformation to β-Si_3N_4. On the other hand, the fine α-Si_3N_4 grains show more rapid transformation to β-Si_3N_4 with attendant grain elongation. The resulting microstructure thereby provides relative homogeneous/heterogeneous microstructures.

Hertzian indentation technique with spherical indenters are used to induce controlled damage patterns.[20,21] Hertzian indentation tests are also used to investigate damage tolerance. Bend tests on damaged bar are carried out to investigate the damage tolerance.[22,23] Contact-induced fracture, damage, and damage tolerance have been focused because contact loading is highly relevant to many structural applications such as bearings, cutting tools, valves, and engine components.

In this paper, a damage-tolerant Si_3N_4 bilayer that suppresses cracks will be described. Bilayer systems with both high hardness and high toughness due to the damage tolerance will be investigated.

II. Experimental Procedure

1. Sample preparation and characterization

The starting silicon nitride powders used in this study were fine α-Si_3N_4 (UBE-SN-E10, average particle size 0.3 μm, Ube Industries, Tokyo, Japan) and coarse α-Si_3N_4 (UBE-SN-E3, average particle size 1 μm, Ube Industries, Tokyo, Japan). Sintering additives were 5 wt% Y_2O_3 (Fine Grade, H. C. Starck GmbH, Goslar, Germany), 2 wt% Al_2O_3 (AKP 50, Sumitomo Chemical Co. Ltd., Tokyo, Japan), and 1 wt% MgO (High Purity, Baikowski Co., N. C. USA). The powders were mixed as a slurry in isopropanol for 24 h in a planetary ball mill, using zirconia balls in a polypropylene container. After drying, the softly agglomerated powder was crushed and sieved through a 60 mesh screen. Hot pressing for the material of each layer was performed in nitrogen gas under uniaxial stress 30 MPa, at 1700°C for 1 h followed by furnace cooling. The bilayer was fabricated at the same temperature, 1700°C, with coating thickness 1 mm and substrate thickness 3 mm. The coarse α-Si_3N_4 powder was packed for the top layer, and the fine α-Si_3N_4 for the substrate layer.

Specimen surfaces normal to the hot press direction were polished to 1 μm finish to enable characterization as well as mechanical testing. These surfaces were plasma etched to highlight the grain structures. The microstructures of the sintered specimens were observed by scanning electron microscopy (SEM).

The elastic modulus of each layer monolith was measured by using a sonic method. In addition, the yield stress of each material was determined by the first incidence of yield.[8] Application of Nomarski illumination enhanced the detection of surface impressions at each given load in the optical microscope. The thermal expansion coefficients of layer monoliths were measured by dilatometer, and α/β phase ratios of the sintered specimen were determined by X-ray diffraction (XRD).[24]

2. Indentation tests

The fired monoliths and bilayers were cut into 3 mm × 4 mm × 25 mm bars for mechanical testing. The top surfaces of the bars were ground to produce a coating thickness of 480, 120, 70, and 40 μm, respectively. Then the specimen surfaces normal to the hot-press direction were diamond-polished to 1 μm finish to enable characterization as well as mechanical testing. Hertzian damage tests across the interface of the side surface were conducted on the bilayer. Indentations were made on the diamond-polished surfaces using tungsten carbide (WC) spheres with a radius of r=1.98 mm, at P=3000 N.

Hertzian indentations were made on each layer as well as on the bilayers, using bonded-interface specimens.[25] The indentations were made symmetrically on the interfaces of the top surfaces using WC spheres with a radius of r=1.98 mm at loads up to P=4000 N. After indentation, the specimens were soaked in acetone to dissolve the adhesive and separate the specimens into two. After cleaning the surfaces, optical microscopy in Nomarski interference contrast was used to observe the subsurface deformation and fracture patterns.

Vickers indentation tests were made on the polished surfaces. A set of Vickers indentation test was made at load P=100 N on the top side of the bilayer with different coating thickness. Hardness, H and toughness, T_O were measured using following equations.[26,27]

$$H = P/2a^2 \tag{1}$$

where, P is indentation load, and a is average value of half-diagonal lengths.

$$T_O = \chi P/c^{3/2} \tag{2}$$

where, χ=0.016 $(E/H)^{1/2}$ with E, elastic modulus and c is indentation crack length.

3. Evaluation of damage tolerance

Some 3 mm × 4 mm × 25 mm specimens were used for strength testing.[22,23] The top surfaces of the bars were ground to produce a coating thickness of 100, 200, and 400 μm. Four point flexural tests were carried out on the Si_3N_4 bilayer as well as coating monolith after Hertzian indentation in universal testing machine. The indentation sites were centered on the tensile side of the bend fixture using WC ball sphere with a radius of r=1.98 mm. The indentation load varied from P=0 to P=4000 N. The bars were broken in fast fracture (<10 msec) and then strengths were calculated.

Cyclic indentations were made with a Hertzian indentation fatigue test.[22] The Si_3N_4 bilayer with a coating thickness of 40 μm were prepared for testing. Silicon nitride (Si_3N_4) sphere with a radius of 1.98 mm was indented on the central region of the tensile side in the bend fixture. Specified maximum load, P=1000 N, was

Fig. 1. Microstructure of Si_3N_4 bilayer. Symbols indicate interface between coating (top) and substrate (bottom) layer.

cyclically delivered using dynamic Instron machine in air environment. Sine wave cycling between minimum (10% of maximum load) and specified maximum loads was conducted at frequencies 10 Hz with an increasing number of cycles, $n=10^0 \sim 5\times10^4$. The bars were also broken in a four point flexural test and strengths were calculated.

III. Results and Discussion

1. Material characterization

Fig. 1 shows the SEM(scanning electron microscopy) micrograph of bilayer. Porosity is not evident in the bilayer and density was confirmed full density (>99%) using the Archimedes method. The coating layer shows a relatively equiaxed microstructure, and the substrate layer contains relatively elongated grains. A discrepancy in the microstructure between the coating and the substrate layer appeared clearly. This microstructural difference is related to the phase transformation rate during sintering. The driving force of sintering in coarse powder is much slower so that more alpha phase remains after sintering. In the coating material, the microstructure consists of mostly α-grains of diameter $\approx$1.2 μm. ($\approx$77 vol%). In the substrate material, the microstructure consists of β-grains (100 vol%). This different phase transformation rate causes the microstructural difference.

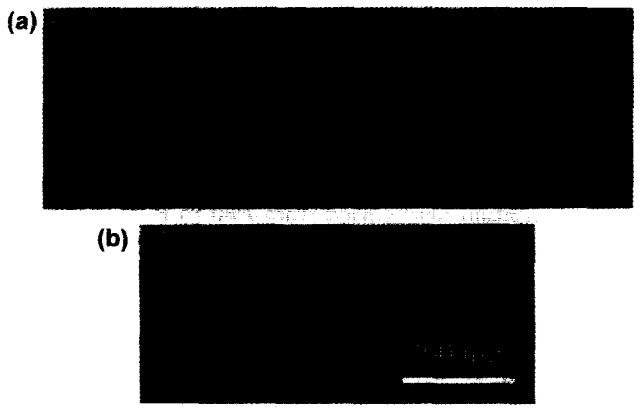

Fig. 2. Contact damage under P=4000 N of (a) coating and (b) substrate monolithic Si_3N_4 material.

Fig. 3. Hertzian indentations on side surface of Si_3N_4 bilayer, made symmetrically across interface at P=3000 N.

Table 1. Characteristics of Coating and Substrate Material

Characteristics	Coating	Substrate
Elastic modulus, E (GPa)	335	315
Yield stress, Y (GPa)	7.9	7.1
Thermal expansion coefficient, α ($\times10^{-6}$/°C)	4.16	4.62

Fig. 2 compares the bonded-interface section views, including contact damages in monolith silicon nitrides from indentation using a WC ball with a radius of 1.98 mm at load P=4000 N. The coating material is very brittle, but the substrate is relatively tough and damage absorbent. In Fig. 2(a), a developed Hertzian cone crack initiated and propagated catastrophically, but the crack was suppressed with microstructural coarsening as shown in Fig. 2(b). Therefore, we confirmed that microstructural tailoring has a strong influence on the contact damage response.

Fig. 3 shows Hertzian indentation across the interface made on the polished section of the side surface. Interface delamination was not shown in this bilayer, indicating a strong interface. Although Hertzian crack appeared in the coating layer, it was suppressed in the substrate because of quasi-ductility as shown in Fig. 2(b). This result provides for the possibility of a damage-tolerant Si_3N_4 bilayer system.

The elastic modulus, yield stress, and thermal expansion coefficient of each monolith are summarized in Table 1. The coating layer material was stiffer than the substrate material. The elastic modulus and yield stress of the coating material were higher, and the thermal expansion coefficient was lower.

2. Indentation results

Contact damage formed in 120 μm coated silicon nitride bilayer is shown in Fig. 4. The damage was formed by Hertzian indentations from a WC ball with a radius

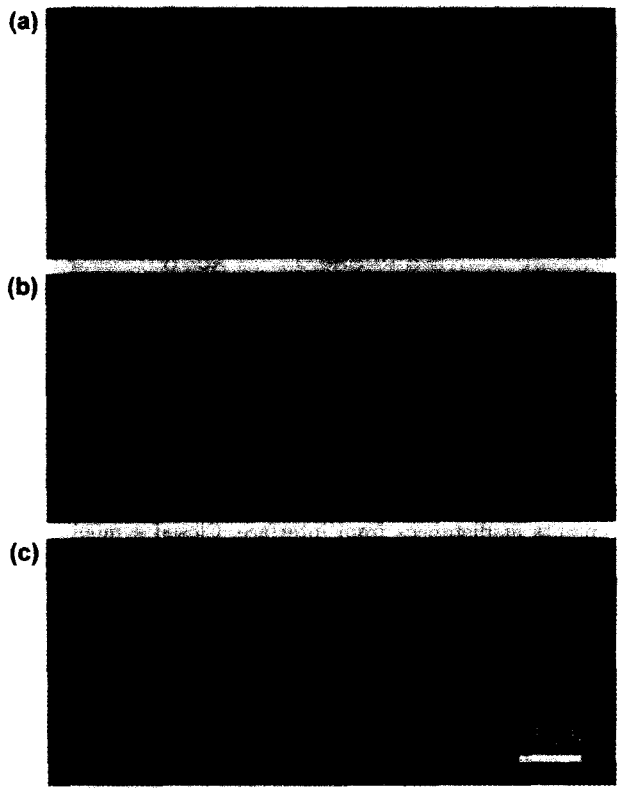

Fig. 4. Contact damage of Si_3N_4 bilayers, fixed coating thickness α=120 μm : at loads (a) P=2000 N, (b) P=3000 N and (c) P=4000 N.

of 1.98 mm. The experimental variable was indentation loads from 2000 to 4000 N. At P=2000 N, a Hertzian crack was initiated in the coating layer from the surface maintaining cone shape. However, the macro-crack was not observed in the substrate, but only a small damage zone was observed. At load P=3000 N, the cone crack propagated further, but was limited to the coating layer, and the size of the damage zone increased. At an higher load, P=4000 N, crack suppression around the interface were more obvious. The Hertzian crack suppression was compared to the crack which popped-in catastrophically as shown in Fig. 2(a). The Hertzian crack did not penetrate the interface and stopped around the interface, extending the damage zone.

The results of Fig. 5 confirm again the fact that the crack was limited to the coating layer. The Hertzian crack was even further suppressed as the coating thickness decreases to 70 and 40 μm. In addition, the size of the damage zone increased with decreasing coating thickness.

The crack suppression was also confirmed by Vickers indentation on the top surface of bilayer. This test was performed on the coating surface of the bilayer at a constant load, P=100 N. The results are shown in Fig. 6. As the coating thickness decreased, the Vickers radial crack length also decreased. This tendency was similar to the results of the Hertzian crack suppression. The toughness

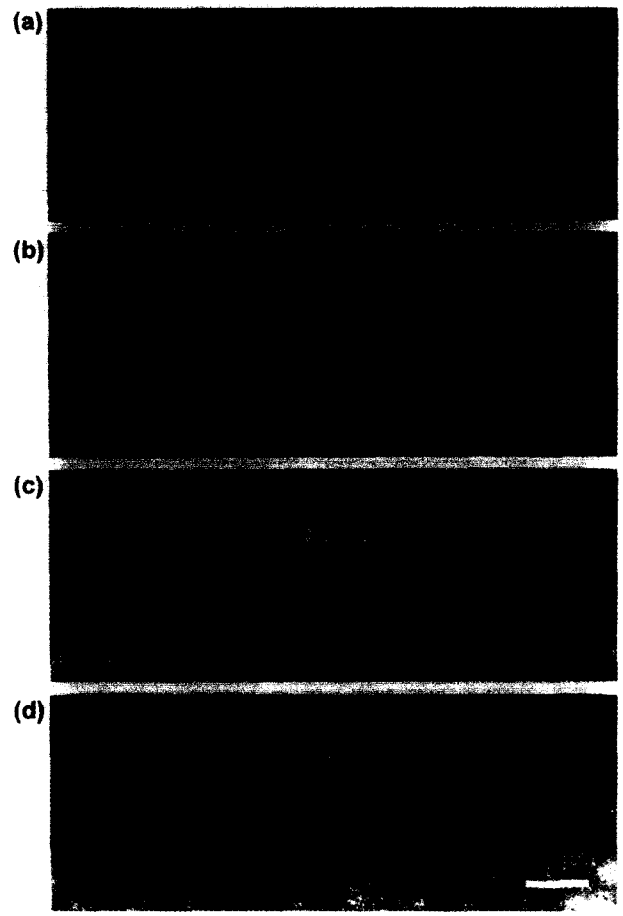

Fig. 5. Contact damage of Si_3N_4 bilayers under fixed load P= 3000 N : at coating thicknesses (a) α=480 μm, (b) 120 μm, (c) 70 μm and (d) 40 μm.

of the bilayer increased up to 5.8 $MPam^{1/2}$ as the coating thickness decreased up to 40 μm and this value was

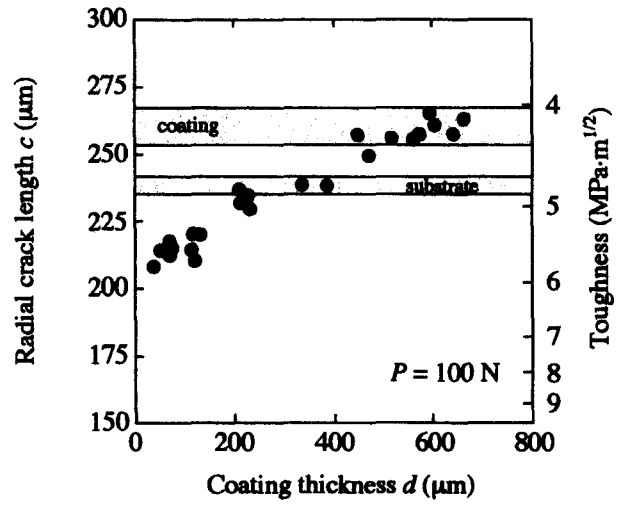

Fig. 6. Vickers radial crack length as function of coating thicknesses in Si_3N_4 bilayer. Toughness data corresponds to that of coating Si_3N_4 material. Boxes indicate radial crack range of coating and substrate Si_3N_4 materials, respectively.

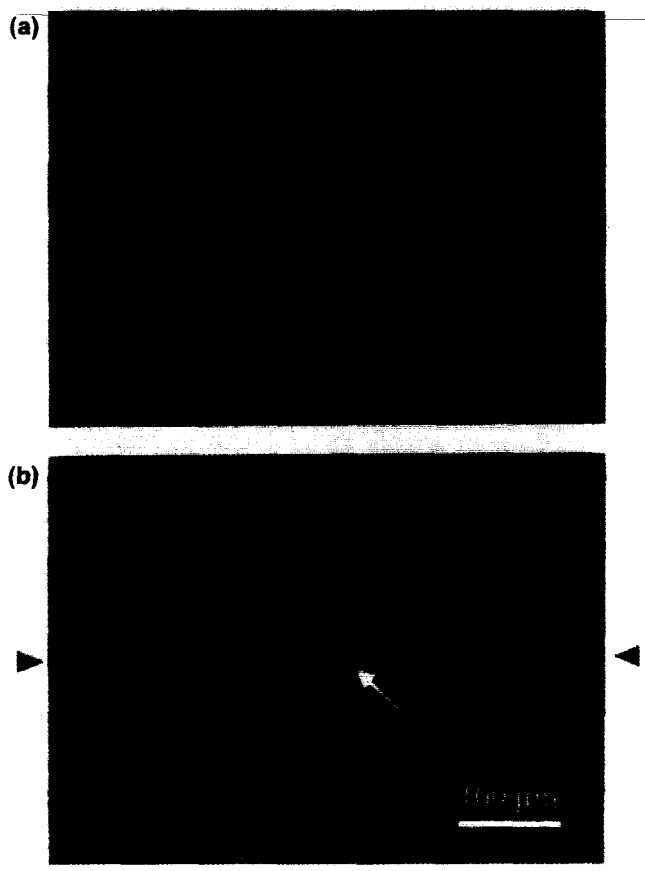

Fig. 7. Micrographs of Vickers radial cracks in the coating layer of Si_3N_4 bilayer : indent site is (a) away from interface and (b) near the interface. Dark symbols indicate interface. Note remarked shorten crack length (white arrow).

higher than that of the substrate monolith (4.8 $MPam^{1/2}$). On the other hand, hardness values ($\simeq$21 GPa) were not changed with coating thickness.

The crack suppression around the interface was confirmed by Vickers experiment on the side polished surface. The indent positions were varied according to the distance from the interface as shown in Fig. 7. When the distance between the interface and the site of the indentation was large ($d \simeq 500$ μm), the radial cracks were similar to each other as shown in Fig. 7(a). However, when the distance was close to the interface, the radial cracks in a normal direction to the interface were suppressed. On the other hand, the radial cracks in a parallel direction to the interface increased (opposite direction). Note the remarked shorter crack length in Fig. 7(b) as compared to that in Fig. 7(a).

Variable radial crack lengths were plotted as a function of variable distance in Fig. 8. The dotted line indicates the interface between the coating and substrate layer. As the distance from the interface decreased in the coating layer, the crack lengths in a normal direction to the interface decreased as shown in Fig. 7.

These results suggest that crack suppression was mostly due to the residual compressive stress in the coating layer.

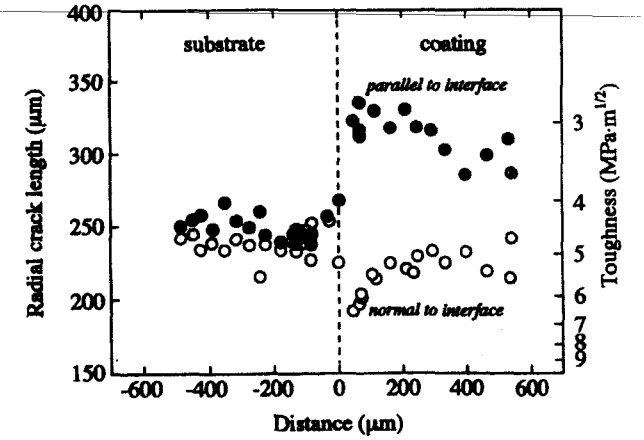

Fig. 8. Plot of radial crack length for Vickers indentations in Si_3N_4 bilayer. Data points are from crack size measurements at distances from interface. Closed symbol denote size of crack parallel to interface. Open symbol denote size of crack perpendicular to interface. Toughness represents that of coating Si_3N_4 monolith material.

The residual stress in the coating layer which was due to the mismatch of thermal expansion coefficients can be estimated by[18]

$$\sigma_R = (\alpha_c - \alpha_s) \cdot \Delta T \cdot \frac{E_c}{(1-\nu_c)+(2h_c/h_s)(E_c/E_s)(1-\nu_s)} \quad (3)$$

where the subscripts c and s indicate the coating and substrate, respectively. α is the thermal expansion coefficient, E is Young's modulus, ν is poisson's ratio, and h is the layer thickness. Assuming $\nu_c=\nu_s=0.27$, ΔT=1430°C (glass crystallization temperature$\simeq$1450°C) and h_s=3000 μm, as E_c, E_s, α_c, and α_s are known values (Table 1), σ_R can be calculated as a function of ratio of coating thickness.

Fig. 9 plots the residual compressive stresses σ_R as a function of coating thickness ratios, dc/ds, from Eq.(3) (curved line). The data points are evaluations from radial crack measurements on the coating sections by Eq.(4),[28]

$$\chi P/c^{3/2} + \psi \sigma_R c^{1/2} = T_O \quad (4)$$

where P is the peak contact load, c is the characteristic crack size, χ is a dimensionless factor which represents the intensity of the persistent field, and ψ is a crack geometry form. Note that the result of stresses from Eq. (3) and stresses from Eq.(4) are well matched to each other. These results show that Hertzian crack suppression was mostly due to the residual compressive stresses by thermal mismatch during cooling.

However, at the same time, the interesting phenomena that a set of secondary crack begins to extend with increasing load or decreasing coating thickness highlight the role of a tough underlayer in suppressing crack propagation in the bilayer structures (Fig. 4(c) or Fig. 5(d)). The Hertzian indentation tests also provide quasi-deformation under the coating/substrate interface. The expansion of the sublayer damage zone as increasing load

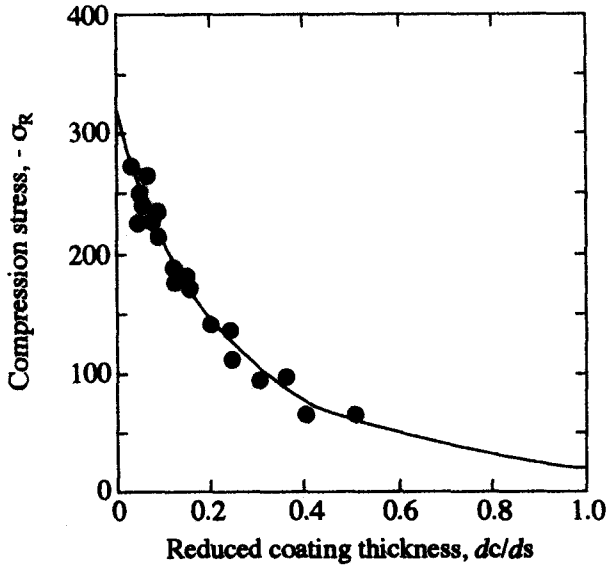

Fig. 9. Residual compression stresses in coatings from thermal expansion mismatch as function of reduced coating thickness dc/ds. Data from Vickers indentation. Solid curve from theoretical fit by thermal expansion mismatch.

and decreasing coating thickness is seen to coincide with the crack suppression, because it is conjectured that deformation within this zone inevitably absorbs mechanical energy, and thereby "shields" the cone crack propagation from the coating layer.

3. Damage tolerance

The results of indentation strength tests for the Si_3N_4 bilayers with different coating thicknesses are shown in Fig. 10. The strengths of the bilayers are plotted as a function of contact load, P, for coating thicknesses d=100 μm, 200 μm, and 400 μm. The data of coating monolith is also included in this figure. Data points are individually

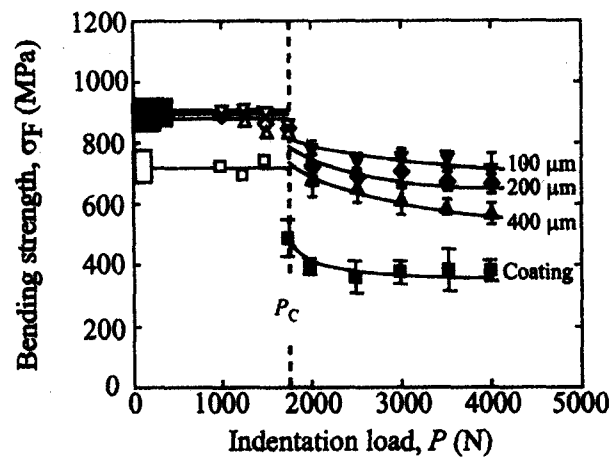

Fig. 10. Strength degradation of Si_3N_4 bilayers for contacts with WC sphere radius r=1.98 mm. Data plotted as a function of indentation load P, for coating thicknesses indicated. Data for coating monolith was included. Solid curves from strength degradation model.[23]

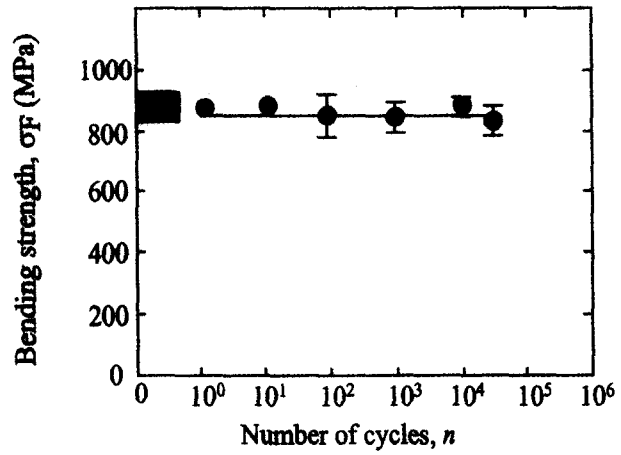

Fig. 11. Strength of Si_3N_4 bilayer as function of number of cycles, after Hertzian indentation at load P=1000 N and frequency 10 Hz. Boxes at left axis represent breaks from specimens without indentations.

measured strengths from indented specimens. Rectangular areas on the left axis represent laboratory strengths σ_o of unindented specimens. Vertical dashed lines represent the critical load P_C for cone cracking in the coating monolith or bilayers. At $P>P_C$, strength values abruptly falloff in the coating monolith and Si_3N_4 bilayers, with failures from cone cracks. However, at $P>P_C$, the strengths data shift strongly upward at thinner coatings. Thus, damage tolerance of the thinner coated Si_3N_4 bilayer is higher than the relatively thick coated bilayer and/or coating monolith.

The results from the measurements of inert strength σ_F of Si_3N_4 bilayer with coating thickness $\simeq$40 μm are plotted as a function of the number of cycle n in Fig. 11. Applied load, P=1000 N, corresponds to beyond the yield point from the Hertzian indentation test, in order to allow for enough development of mechanical damage during cycling. However, relative to the specimens without the cycling test (box at left axis in figure), strength degradation does not occur in the bilayer, which indicates there is no degradation due to wear or low fatigue resistance. No degradation relative to the unindented specimens denotes this Si_3N_4 bilayer has damage tolerance at the given contact loading condition. The results suggest hard/soft Si_3N_4 bilayer structure provides high wear or fatigue resistance with high damage tolerance caused by Hertzian crack suppression.

IV. Conclusion

A hard/soft silicon nitride bilayer with different microstructures was fabricated by hot pressing at 1700°C, 1 hr, under 30 MPa. The hard coating layer consisted of mostly equiaxed and α phase and showed high hardness. On the other hand, the soft substrate layer had β phase with an elongated microstructure and showed high toughness and the damage tolerance.

Hertzian crack propagation could be suppressed by optimum design of elastic/plastic mismatch and coating thickness. The crack suppression was also confirmed by the Vickers indentation test. Hertzian crack suppression results mostly from residual compressive stress in the coating layer and increased quasi-plastic yield in the substrate layer.

Moreover, the suppression of crack propagation in the appropriately designed bilayer diminished the strength loss even under the high or multiple damages. Both high fatigue resistance and damage tolerance were achieved in the bilayer.

Acknowledgement

This cooperative research was sponsored by CISEM (Center for Interface Science and Engineering of Materials) in KAIST.

References

1. B. R. Lawn, Fracture of Brittle Solids, pp.12-14, Cambridge Univ. Press, Cambridge, ed. 2, 1993.
2. T. L. Anderson, Fracture Mechanics, pp.33-36, CRC press, London&Tokyo, 1995.
3. N. McN. Alford, J. D. Birchall and K. Kendall, "High-Strength Ceramics through Colloidal Control to Remove Defects," *Nature,* **330**(5), 51-53 (1987).
4. S. J. Bennison, N. P. Padture, J. L. Runyan and B. R. Lawn, "Flaw-Insensitive Ceramics," *Phy. Mag. Lett.,* **64** (4), 191-195 (1991).
5. N. P. Padture, S. J. Bennison and H. M. Chan, "Flaw Tolerance and Crack Resistance Properties of Alumina-Aluminum Titanate Composites with Tailored Microstructures," *J. Am. Ceram. Soc.,* **76**(9), 2312-2320 (1993).
6. B. R. Lawn, N. P. Padture, L. M. Braun and S. J. Bennison, "Model for Toughness Curves in Two-Phase Ceramics : I. Basic Fracture Mechanics," *J. Am. Ceram. Soc.,* **76**(9), 2235-2240 (1993).
7. N. P. Padture, J. L. Runyan, S. J. Bennison, L. M. Braun and B. R. Lawn, "Model for Toughness Curves in Two-Phase Ceramics: II. Microstructural Variables," *J. Am. Ceram. Soc.,* **76**(9), 2241-2247 (1993).
8. S. K. Lee, S. Wuttiphan and B. R. Lawn, "Role of Microstructure in Hertzian Contact Damage in Silicon Nitride : I. Mechanical Characterization," *J. Am. Ceram. Soc.,* **80**(9), 2367-2381 (1997).
9. D. D. Lee, S.-J. L. Kang, G. Petzow and D. N. Yoon, "Effect of α to β Phase Transition on the Sintering of Silicon Nitride Ceramics," *J. Am. Ceram. Soc.,* **73**, 767-769 (1990).
10. M. Mitomo, M. Tsutsumi, H. Tanaka, S. Uenosono and F. Salto, "Grain Growth during Gas-Pressure Sintering of β-Silicon Nitride," *J. Am. Ceram. Soc.,* **73**(8), 2441-2445 (1990).
11. S. K. Lee, K. S. Lee, B. R. Lawn and D. K. Kim, "Effect of Starting Powder on Damage Resistance of Silicon Nitrides," *J. Am. Ceram. Soc.,* **81**(8), 2061-2071 (1998).
12. H. H. K. Xu, L. Wei, N. P. Padture, B. R. Lawn and R. L. Yeckley, "Effect of Microstructural Coarsening on Hertzian Contact Damage in Silicon Nitride," *J. Mater. Sci.,* **30**, 869-879 (1995).
13. H. M. Chan, "Layered Ceramics : Processing and Mechanical Behavior," *Ann. Rev. Mater. Sci.,* **27**, 249-282 (1997).
14. S. Baskaran, S. D. Nunn, D. Popovic and J. W. Halloran, "Fibrous Monolithic Ceramics : I. Fabrication, Microstructure and Indentation Behavior," *J. Am. Ceram. Soc.,* **76**(9), 2209-2216 (1993).
15. W. J. Clegg, K. Kendall, N. M. Alford, T. W. Button and J. D. Birchall, "A Simple Way to Make Tough Ceramics," *Nature,* **347**, 455-457 (1991).
16. O. Prakash, P. Sarkar and P. S. Nichoson, "Crack Deflection in Ceramic/Ceramic Laminates with Strong Interfaces," *J. Am. Ceram. Soc.,* **78**(4), 1125-1127 (1995).
17. A. V. Virkar, J. L. Huang, R. A. Cutler, "Strengthening of Oxide Ceramics by Transformation-Toughened Alumina by Selective Phase Transformation," *J. Am. Ceram. Soc.,* **70**, 714-718 (1987).
18. H. Wang and X. Hu, "Surface Properties of Ceramic Laminates Fabricated by Die Pressing," *J. Am. Ceram. Soc.,* **79**, 553-556 (1996).
19. K. S. Lee, S. Wuttiphan, X. Z. Hu, S. K. Lee and B. R. Lawn, "Contact-Induced Transverse Fractures in Brittle Layers on Soft Substrates : A Study on Silicon Nitride Bilayers," *J. Am. Ceram. Soc.,* **81**(3), 571-580 (1998).
20. B. R. Lawn, N. P. Padture, H. Cai and F. Guiberteau, "Making Ceramics 'Ductile'," *Science,* **263**, 1114-1116 (1994).
21. F. Guiberteau, N. P. Padture and B. R. Lawn, "Effect of Grain Size on Hertzian Contact Damage in Alumina," *J. Am. Ceram. Soc.,* **77**(7), 1825-1831 (1994).
22. F. Guiberteau, N. P. Padture, H. Cai and B. R. Lawn, "Indentation Fatigue : A Simple Cyclic Hertzian Test for Measuring Damage Accumulation in Polycrystalline Ceramics," *Phil. Mag. A.,* **68**(5), 1003-1016 (1993).
23. B. R. Lawn, S. K. Lee, I. M. Peterson and S. Wuttiphan, "Model of Strength Degradation from Hertzian Contact Damage in Tough Ceramics," *J. Am. Ceram. Soc.,* **81**(6), 1509-1520 (1998).
24. C. P. Gazzara and D. R. Messier, "Determination of Phase Content of Si_3N_4 by X-Ray Diffraction Analysis," *Am. Ceram. Soc. Bull.,* **56**(9), 777-780 (1977).
25. H. Cai, M. A. S. Kalceff and B. R. Lawn, "Deformation and Fracture of Mica-Containing Glass-Ceramics in Hertzian Contacts," *J. Mater. Res.,* **9**(3), 762-770 (1994).
26. D. Tabor, Hardness of Metals, Clarendon, Oxford, (1951).
27. D. B. Marshall, T. Noma and A. G. Evans, "A Simple Method for Determining Elastic Modulus-to-Hardness Ratios Using Knoop Indentation Measurements," *J. Am. Ceram. Soc.,* **65**(10), C175-176 (1982).
28. B. R. Lawn, E. R. Fuller, Jr., "Measurement of Thin-Layer Surface Stresses by Indentation Fracture," *J. Mat. Sci.,* **19**, 4061-4067 (1984).